Optimizing the bumper beam and crash box of a vehicle with shape memory alloys for crashworthiness

Mohab Elmarakbi, Ahmed Elmasry, Yongqing Fu, and Ahmed Elamrakbi

Faculty of Engineering and Environment, Northumbria University Newcastle Upon Tyne, NE1 8ST, UK

Abstract

Shape memory alloys (SMAs) present an interesting opportunity. The ability for the SMA to change its shapes/properties due to an external trigger allows a great potential in improving the crash worthiness of vehicles, which links to their ability to withstand a collision to protect drivers from injury in the event of a crash. For this crash worthiness study, SMA wires will be incorporated into the design to form various front-end components of a vehicle such as the bumper beam and crash box. The modelling of crash worthiness testing will be conducted using LS-DYNA software. The SMAs will be used in the form of wires and combined with the standard design for a crash box these SMA wires are modelled using MAT30 material card within LS-DYNA the final design of the bumper beam and crash box components will then be integrated within a standard front-end of vehicle and simulated against realistic crash scenarios to validate crash worthiness of the components with SMA integrated. The optimised designs for the bumper beam and crash box that have shown to have significantly improved the crashworthiness of a frontal collision by of 45% when compared to a standard design moreover side collisions were improved by 44%. These optimised designs also reduced the overall cost by 17% when compared to the original front end structure and more importantly reduced the weight of structures by 75%.

1 Introduction

The ever-increasing demand for lightweight of vehicles means that throughout the years most components of a vehicle have undergone optimization to maximize their weight reduction. However, the demand for light weight components has further been increased, which is mainly due to the shift of focus to electric vehicles. Their large batteries present a massive weight issue, leaving manufactures looking for further components to optimize to reduce the overall weight of the vehicle to accommodate the batteries required. However, there is a critical issue concerning the tradeoff problem between weight reduction and structural integrity, which means that components such as the front-end structure of the vehicle have remained relatively untouched due to the inability to compromise safety for these components. There have been many postulated methods in optimizing the crash worthiness of the front-end structure of an automotive vehicle, either changing the materials used, altering the physical from of the structures, or adding a new component. For instance, Li et al. (2017) used aluminum alloy 6060, TRIP800 and DP800 for the bumper, crash box, and front rail, respectively, nstead of steel (Liu and Ding, 2016). They reported that this change in material offered a 10.1% increase in energy absorption with an 11.1% decrease in overall Mass. For another example, redesigning and optimizing the vehicle structures offers an increase in weight reduction by 7% in an all-steel vehicle whilst the decrease of mass is between 30-50% with an all-aluminum vehicle (Jambor and Beyer, 1997). However, weight reduction above 50% can only be achieved using a composite design (Elmarakbi et al. 2020). Thermoplastic polymer-based glass fibre composite, more specifically SGF PA6, has been used within the crash box to improve crash worthiness (Elmarakbi et al. 2017). It was found that the composite reduced the primary peak force and had a similar specific energy absorption result as the same crash box with steel as the utilised material (Elmarakbi. et al. 2017). Furthermore, the addition of GnPls was added to this SGF/PA6 composite at 2% (Elmarakbi. et al. 2017). This increased the specific energy absorption (SEA) drastically whilst also decreasing peak force when compared to the steel version

of the same crash box (Elmarakbi et al. 2017). Various methods of integration and utilization for SMAs have been explored, the most prevalent material used for shape memory alloys is nickel-titanium (NiTi). It has high wear and corrosion resistance, and more importantly, it has extraordinary properties such as super elasticity and shape memory effect (Nair and Nachimuthu, 2022). A shape memory alloy has two phases, i.e., the austenite phase and the martensite phase. When the SMA is cooled, it enters its martensite phase where the SMA can be deformed into many different shapes. Once the SMA is heated again above the austenite transformation temperature, it returns to its original shape. Modeling the SMA has been conducted using LS-DYNA. The simulations mainly use two ways, (1) creating a user material card (UMAT), or (2) using one of the two available materials cards within the program, MAT30 and MAT291. While the MAT30 is developed based upon the assumption of generalized plasticity, but the MAT291 is developed by minimizing a single energy problem which describes all the phase transformations possible, thus the energy problem minimizes is the Helmolt'z free energy potential. (Karlsson et.al, 2019).

2 Materials & Methods

The focus of optimization will focus on two of the primary components of the front-end structure, which are the crash box and bumper. The optimization was focused on two of the primary components of the front-end structure, which are the crash box and bumper. The optimization was done by changing the material and incorporating SMA. The use of SMA reduces the weight of the components drastically whilst maintaining and improving the crashworthiness of the components. When modelling the front-end structure and optimizing the crash box, it is essential to maintain specific conditions, so the results will not be dramatically changed. The bumper beam was modelled using steel and the simulation parameters are obtained from Sun et al. 2018. The research presented by Rao et al. (2016) and that of Acar et al. (2020) modelled the bumper beam with very similar parameters. Furthermore, this also applied to the crash box that will undergo the optimization, thus a standard crash box was utilized which was obtained from Ried, 2022. Once the components were obtained and created, the parameters of FEA and simulations are needed to be configured to define both the element size of the mesh and the number of integration points. The element size of the mesh utilized for the various models was obtained by conducting a mesh sensitivity analysis (MSA). The mesh analysis conducted for this project was consisted of varying the mesh size from 1-15 in increments of 1. The deflection of each simulation the value for the element size identified was 5, as this was the value were the deflection started to plateau. Similarly, the nodal points of integration (NIP) were obtained via trial and error and the ideal NIP was found to be 10. The FEA environment developed for simulating the crash box compression was consisted of fixing the nodes at one end of the crash box using specific boundary conditions (SPC) and implementing a rigid wall, more specifically a PLANAR_MOVING_FORCES rigid wall, at the other end to conduct the impact. The impact simulated a realistic crash scenario by consisting of a mass of 800 kg and a traveling speed at 20 mph (Elmarakbi et. al, 2017). The materials used during simulation were, steel, a composite consisting of short S-glass fiber (SGF) 60%, thermoplastic polymer (PA6) 40% and graphene nanoplates (GnPls) 2% loading in weight (wt.%) and Nickel-Titanium (NiTi). The standard crash box and bumper consisted of steel, this would also in turn form the basis for comparison when altering the materials and implementing the shape memory alloys (SMA). Furthermore, the NiTi, is the most implemented SMA which for this use case is integrated to further improve the crashworthiness whilst maintaining practically all the wight reduction gained by implementing the SGF/PA6/GnPls. The mechanical properties for steel were obtained from ASTM,1990. Whilst the mechanical properties for the nickel-titanium (NiTi) were obtained from Matthey, 2023. The mechanical properties for SGF/PA6/GnPls were obtained from Elmarakbi et. Al 2022.The NiTi was implemented into the created models within LS-DYNA using material card 30 (MAT_SHAPE_MEMORY (030)). This is due the model being compromised of shell elements whilst MAT_291 is more suited to solid elements. Furthermore, the mechanical properties of the SMA NiTi were obtained from its data in a martensite phase.

This assumption is that the SMA has not received a thermal stimulation to activate into the austenite. By modeling it in the martensite, a baseline of improvement can be obtained ensuring if the SMA has been or not been activated for any reason that in its base form it will still ensure occupant safety.

Table 1: Material Cards used for each Material.

Material	Material Card
Steel	MAT_PIECEWISE_LINEAR_PLASTICITY (024)
NiTi	MAT_SHAPE_MEMORY (023)
SGF/PA6/GnPls	MAT_ENHANCED_COMPOSITE_DAMAGAE (054/055)

There are two main SMA wire composite configurations, as shown in Fig. 1. Each is consisted of wires with a diameter of 0.5 mm and a length of 272 mm. Five SMA wires were added to a single side of the crash box. For the first arrangement, two faces of the crash box were embedded with SMA wires totaling to 10 wires used. The second arrangement had all four faces of the crash box layered with these wires with 20 wires being used all together.

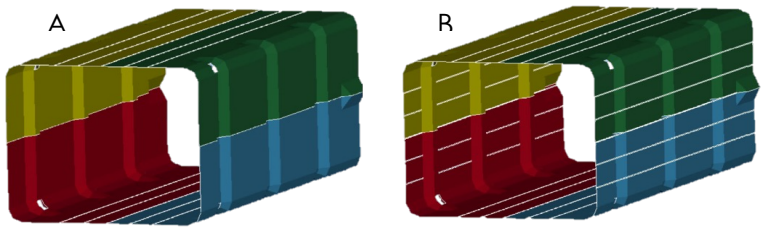

Figure 1: SMA Arrangements, A) 2 face arrangement and B)4 Face Arrangement

The selected crash box was then combined with the bumper beam, then the optimization under real world-conditions was simulated. Two collision scenarios were simulated, a frontal collision as well as a side collision.

3 Results & Discussion

Table 2: Weight Comparison of Crash boxes

Properties	Mass (kg)
Steel Crash Box	1.746
SGF/PA6/GnPls Crash Box	0.435
SGF/PA6/GnPls Crash Box with 10 SMA Wires	0.439
SGF/PA6/GnPls Crash Box with 20 SMA Wires	0.444

Table 3: Weight Comparison of the various Front-end structures (FES)

FES Design	Mass (kg)
Standard Design with Steel	20.973
Standard Design with SGF/PA6/GnPls	5.247
SMA integrated Design with SGF/PA6/GnPls	5.255

Table 2 shows that when the material of the crash box was changed from steel to SGF/PA6/GnPls, the **weight was reduced by 75%.** When the SMAs were introduced, the weight was increased slightly than the crash box made of only SGF/PA6/GnPls. The increase in weight was 0.0015% when 10 SMA wires was added, and that value was 0.0030% when 20 SMA wires were introduced. However, these values are nearly negligible in the weight reduction thus overall, the various crash box was maintained approximately a 75% weight reduction when compared to the steel version. This 75% weight reduction is also observed when comparing the modified FES to the standard design with steel FES as listed in Table 3.

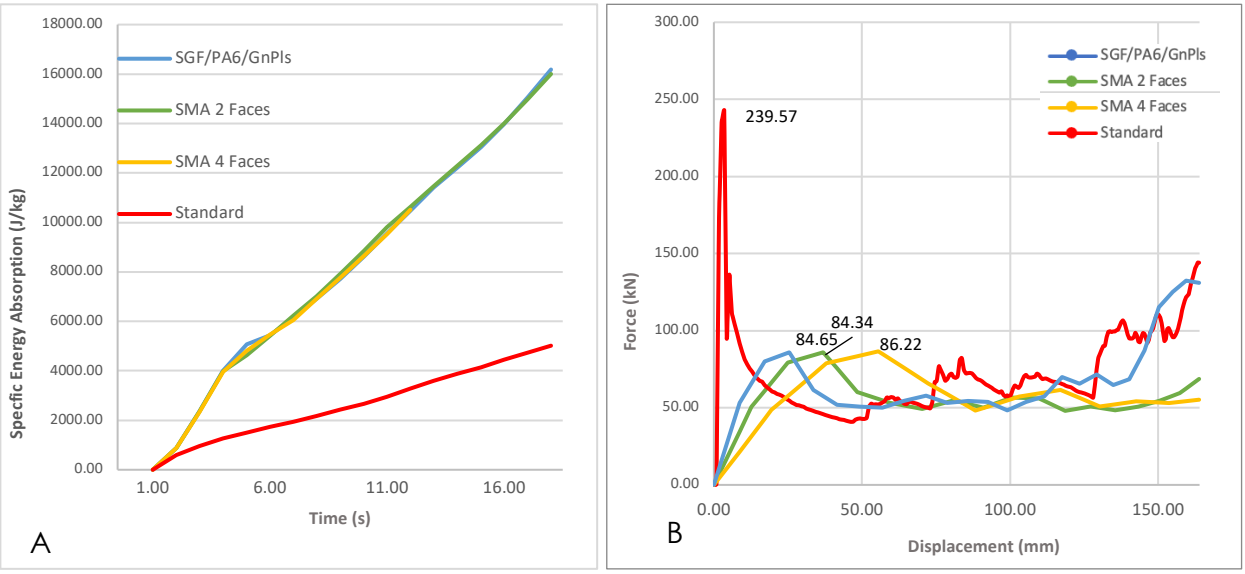

Figure 2: A) Specific energy absorption (SEA) comparison of the various crash box designs and B) Force against displacement comparison of the various crash box designs

Figure 2A shows that all the modified cashboxes reduced the peak force when compared to the crash box made of steel. The **overall increase in SEA is 69%** when compared to the steel version. Figure 2B, presents the force against displacement for the various crash boxes modelled. It shows that all the modified designs show lower peak forces compared with those of the baseline steel crash box with the standard design. In addition, the two faced SMA wire design showed the lowest peak force by a slight margin, whereas all the various modified designs are observed to have a similar **decrease in their peak force of roughly 65%.** Moreover, the two faced SMA design prevents the second deacceleration pulse observed when the material was changed from steel to SGF/PA6/GnPls.

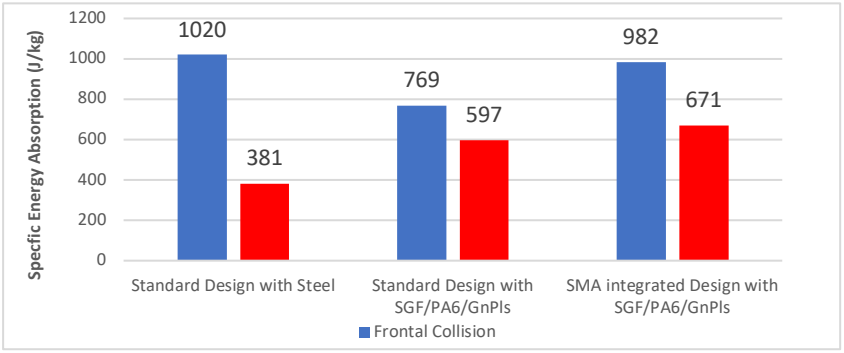

Figure 3: SEA comparison of the various FES structures

When the crash boxes were implemented with the bumper beam to simulate a front-end structure (FES), three version were modelled: 1. Standard design with steel FES, 2. Standard Design with SGF/PA6/GnPls and 3. SMA integrated Design with SGF/PA6/GnPls. These three FES designs were then simulated under realistic collision scenarios and the SEA of both front and side collisions were compared for each FES design, with the obtained results shown in Fig.3. In addition, Fig. 3 shows that the SEA values of the standard design with SGF/PA6/GnPls had a decrease of 25% when compared to the baseline of standard design with steel FES. However, the SEA was increased during a side collision by 36%. The SMA integrated design with SGF/PA6/GnPls increased the SEA of a frontal collision when compared to the standard design with SGF/PA6/GnPls by 22%. **When compared to the standard design with steel, there was now only a decreased of 0.04%.** This means that the SMA integrated design was able to drastically reduce the weight whilst maintaining the structural integrity and crashworthiness during a frontal impact. In addition, the SMA integrated design with SGF/PA6/GnPls increased the SEA during a side collision when compared to the standard design with steel by 43%

Table 4: Peak force Comparison between the various FES designs

FES Design	Frontal Collision Peak Force (kN)	Side Collision Peak Force (kN)
Standard Design with Steel	127.01	41.68
SMA integrated Design with SGF/PA6/GnPls	70.03	23.41

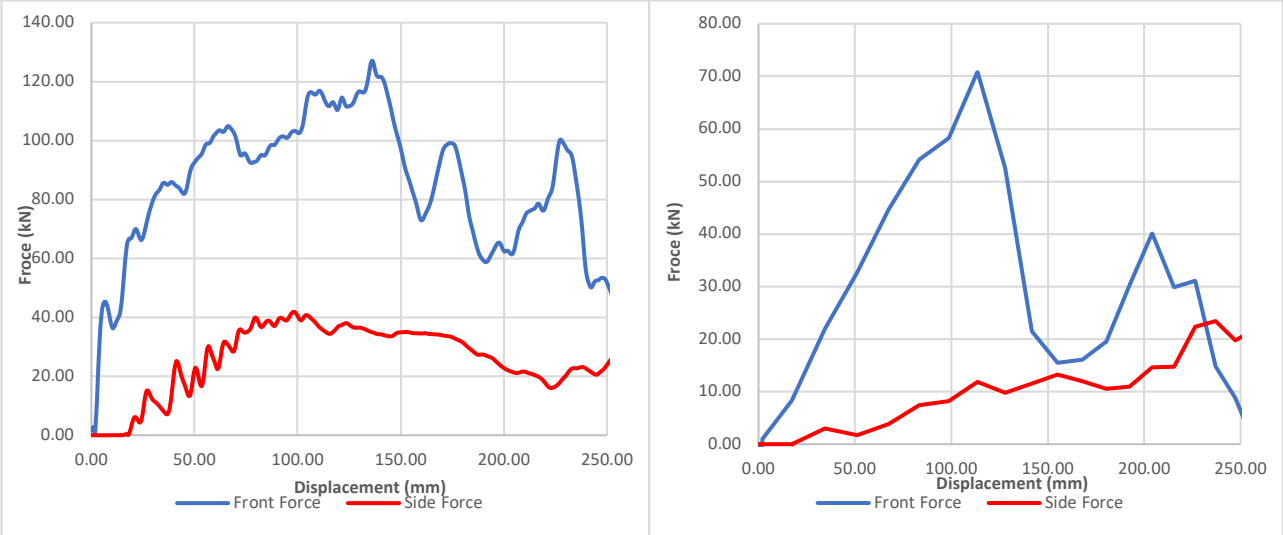

Figure 4: A) Force against displacement comparison for Standard Design with Steel FES and B) Force against displacement comparison for SMA integrated Design with SGF/PA6/GnPls FES

The initial **peak force when compared to the standard design with steel is decreased by 45%** by the SMA integrated design. Furthermore, the SMA integrated design shows that the impact during a side collision is controlled when compared than the standard design with steel, which indicates its increased crashworthiness and thus the improvements in occupant's safety. Furthermore, the peak force of the SMA integrated design **decreases the peak force of a side collision by 44%** when compared to the standard design with steel.

4 Conclusion

Integration of SMA into designs of both the crash box and FES was able to reduce the weight by 75% in comparison to a standard design using steel. This weight reduction didn't reduce the structural integrity or crashworthiness, but instead increased the peak force during a frontal collision by 45% and during aside collision by 44%. Even when the SMA isn't activated the crashworthiness is still effective, thus ensuring occupant safety even in a worst-case scenario that the SMA is not activated in time of the collision.

Acknowledgments

The research leading to these results has received funding from the Horizon EU Programme under grant agreement No. 10047227 and UKRI grant agreements No. 10047227 and No.10047305 (SALIENT Project).

References

1. ASTM International. (1990) "Metals Handbook, Vol.2- Properties and Selection: Nonferrous Alloys and Special Purpose Materials". 10th Ed.
2. Elmarakbi, A., Azoti, W., Serry, M. (2017) "Multiscale modelling of hybrid glass fibres reinforced graphene platelets polyamide PA6 matrix composites for crashworthiness applications" Applied Materials Today, 6, pp.1-8
3. Elmarakbi, A., Ciardiello, R., Tridello, A., Innocente, F., Martorana, B., Bertocchi, F., Cristiano, F., Elmarakbi, M. and Belingardi, G. (2020) "Effect of graphene nanoplatelets on the impact response of a carbon fibre reinforced composite" Materials Today Communications. 25, 101530, pp. 1-11.
4. Elmarakbi, M, Combrinck, M, Elmasry, A, & Elmarakbi, A. "Design of a New Vehicle Front End Structure to Optimise Crashworthiness." Proceedings of the ASME 2022 International Mechanical Engineering Congress and Exposition. Volume 9: Mechanics of Solids, Structures, and Fluids; Micro- and Nano-Systems Engineering and Packaging; Safety Engineering, Risk, and Reliability Analysis; Research Posters. Columbus, Ohio, USA. October 30–November 3, 2022. V009T14A006. ASME. https://doi.org/10.1115/IMECE2022-95911
5. Jambor, A. and Beyer, M. (1997) "New cars - new materials" Materials and Design, 18(4-6), pp. 203-209.
6. Karlsson, J. et al. (2019) 12th European LS-Dyna Conference, Dynalook. Available at: https://www.dynalook.com/conferences/12th-european-ls-dyna-conference-2019
7. Li Zhaokai, Yu Qiang, Zhao Xuan, Yu Man, Shi Peilong and Yan Cilei. (2017). Crashworthiness and lightweight optimization to applied multiple materials and foam-filled front-end structure of auto-body. Advances in Mechanical Engineering. 9. 168781401770280. 10.1177/1687814017702806.
8. Li, Z., Yu, Q., Zhao, X., Yu, M., Shi, P. and Yan, C. (2017) "Crashworthiness and lightweight optimization to applied multiple materials and foam-filled front-end structure of auto-body" Advances in Mechanical Engineering. 9(8), pp.1-21.
9. Liu, Y. and Ding, L. (2016) "A Study of Using Different Crash Box Types in Automobile Frontal Collision" *International Journal of Simulation: Systems, Science and Technology.* 17(38), 21.1-21.5.
10. Matthey, J. (2023) Nitinol-technical-properties, matthey.com. Available at: https://matthey.com/products-and-markets/other-markets/medical-components/resource-library/nitinol-technical-properties
11. Nair, VS., Nachimuthu, R. (2022) The role of NiTi shape memory alloys in quality-of-life improvement through medical advancements: A comprehensive review. Proc Inst Mech Eng H. Jul;236(7):923-950. doi: 10.1177/09544119221093460. Epub 2022 Apr 29. PMID: 35486134.
12. Reid, J. (2022). Crashbox. [online] "Welcome to LS-DYNA Examples". Available at: <https://www.dynaexamples.com/introduction/intro-by-j.-reid/crashbox>
13. Rao, S., Viswatej, k. and Adinarayana, S. (2016) "Design and Sensitivities Analysis on Automotive Bumper Beam Subjected to Low Velocity Impact." *International Journal of Engineering Trends and Technology,* 37, pp. 110-121.
14. Sun, G., Tian, J., Liu, T., Yan, X. and Huang, X. (2018) "Crashworthiness optimization of automotive parts with tailor rolled blank" Engineering Structures. 169, pp. 201-215.